



# Debris-flow surges of a very active alpine torrent : a field database

Suzanne Lapillonne<sup>1</sup>, Firmin Fontaine<sup>1</sup>, Frédéric Liebault<sup>1</sup>, Vincent Richefeu<sup>2</sup>, and Guillaume Piton<sup>1</sup>

<sup>1</sup>Univ. Grenoble Alpes, INRAE, CNRS, IRD, Grenoble INP, IGE, Grenoble, France

<sup>2</sup>Univ. Grenoble Alpes, 3SR, Gières, France

**Correspondence:** Lapillonne Suzanne, (suzanne.lapillonne@inrae.fr)

**Abstract.** This paper presents a protocol to analyze debris flow focusing on the surge scale rather than the full scale of the debris flow event, as well as its application to a French site. Providing bulk surge features like volume, peak discharge, front height, front velocity and Froude numbers allows for numerical and experimental debris flow investigations to be designed with narrower physical ranges and thus, for deeper scientific questions to be explored. We suggest a method to access such features at surge scale that can be applied to a wide variety of monitoring stations. Requirements for monitoring stations for the protocol to be applicable include (i) a flow stage measurements, (ii) a cross section hypothesis and (iii) a velocity estimation. Raw data from three monitoring stations on the Réal torrent (drainage area: 2 km<sup>2</sup>, South-East France) are used to illustrate an application on 34 surges measured from 2011 to 2020 on the three monitoring stations. Volumes of debris-flow surges on the Réal Torrent are typically sized at a few thousand cubic meters. Peak flow height of surges range from 1 to 2 m. Peak discharge range around a few dozens cubic meters per second. Finally, we show that Froude numbers of such surges are near critical.

## 1 Introduction

The destructive nature of debris flows, as well as their sporadic behaviour, make precise debris-flow measurements in the field difficult. Monitoring of debris flow was pioneered in the 1970s (e.g., in Japan, Suwa et al., 2011) and more monitoring stations have developed in the past 20 years (Hürlimann et al., 2019), allowing a wide range of debris-flow events in different torrent morphology to be monitored. In their review, Hürlimann et al. (2019) show the various designs of the monitoring stations and their different objectives. Debris flow monitoring is performed for various purposes including understanding debris flow initiation (Bel, 2017), increasing knowledge on the physics of the flows (Theule et al., 2017), and on impact forces (Nagl et al., 2020).

However, despite years of efforts in monitoring these phenomena, very few data on debris flows had been shared in open databases. The collective effort and interest to gather such data would benefit from a structured method and definition of features of interest. One of the only available datasets was published by McArdell and Hirschberg (2020) who provided dates and bulk volumes of 75 debris-flow events measured on the Illgraben catchment in Switzerland. Comiti et al. (2014) also made available volumes, velocities, and dates of two events measured on the Gadria catchment in Italy as an initial analysis, with the same intent as the present work, namely to formalize and centralize data on debris flow processes. A couple of other events that occurred on the same catchment were also described by Theule et al. (2018) and by Nagl et al. (2020). Guo et al. (2020) made available velocities, flow depth, flow rate, flow width and duration of 23 surges on the Jiangjia Gully in China. Other data



on debris flow features can be found for the Chalk Cliff catchment in the United States (6 events by McCoy et al., 2012) and one event on the Cancia catchment in Italy (Simoni et al., 2020). These few interesting initiatives pave the way to community-driven open databases, they were however extracted from raw data with various approaches making difficult to pool them in a single consistent dataset.

Meanwhile, numerical methods improved tremendously in the recent years. Applications for debris-flow hazard mapping and design of mitigation measures are increasingly attracting attention, and allow always more scientific questions to be answered (Jakob and Hungr, 2005). These methods are now mature enough to model parts of the complex phenomena observed in the field at multiple scales. However, the lack of comparable, relevant, openly available, field data slows down the progresses in performing more realistic debris-flow modeling. This leads to a disparity between field reality and numerical and laboratory experiments. There is, for instance, a habit of exploring very large ranges of Froude numbers in numerical studies of impact forces, typically 1 - 8 (e.g., Albaba et al., 2015; Ceccato et al., 2018; Ng et al., 2020, among others). Performing such extensive parameter studies is a prudent approach that ensure to cover the poorly known variability of Nature. However, it creates huge needs regarding experimental effort, computational power and time. These efforts are a high price to pay as they mean that more complicated scientific questions are not explored due to a lack of resources. In addition, in both experimental and numerical simulations, Froude numbers used are usually high, namely typically  $> 2 - 4$  (e.g., Ng et al., 2020; Chen et al., 2020; Goodwin and Choi, 2022). Meanwhile, various regimes of impacts and flow behavior emerge depending on the Froude number (Faug et al., 2012), but the transition seem to occur for lower Froude values, typically near critical (Laigle and Labbe, 2017). Whether it makes sense to study each regime highlighted in laboratory experiments for field application should be decided in the light of field measurements. Thus, a database would ensure using features that are more representative of field reality, saving time to focus on deeper scientific questions.

Now that monitoring stations have been installed for a reasonable period of time, raw data processing is possible in order to build a common and open data base on flow characteristics of debris-flow surges. Such a database would aim to give access to the scientific community to values of typical flow features such as volume, maximal flow height, peak discharge and Froude numbers of real debris flows. A protocol for debris-flow surges data processing is described in the present paper to focus on the surge scale rather than full scale debris-flow event (several fronts and surges with intermediate diluted flows).

The end goal of this paper is to define a common protocol that is sufficiently simple to apply to make it widely usable to any debris flow monitoring stations. Using it will then permit gathering characteristics of debris-flow surges in a homogeneous, easy to access database. Surge identification, velocity computation and volume determination methods are more thoroughly described in this paper. The protocol we used to process monitoring data is first presented in this paper. Its application to the three monitoring stations of the Réal catchment in South-East France is then explained. The results describe the values of the surge parameters and show synthetically the interest of having several stations on a catchment. The ranges features of surges are first put into perspective with the literature. Potential relationships and evolution of surge features are then investigated and conclusive remarks are drawn.

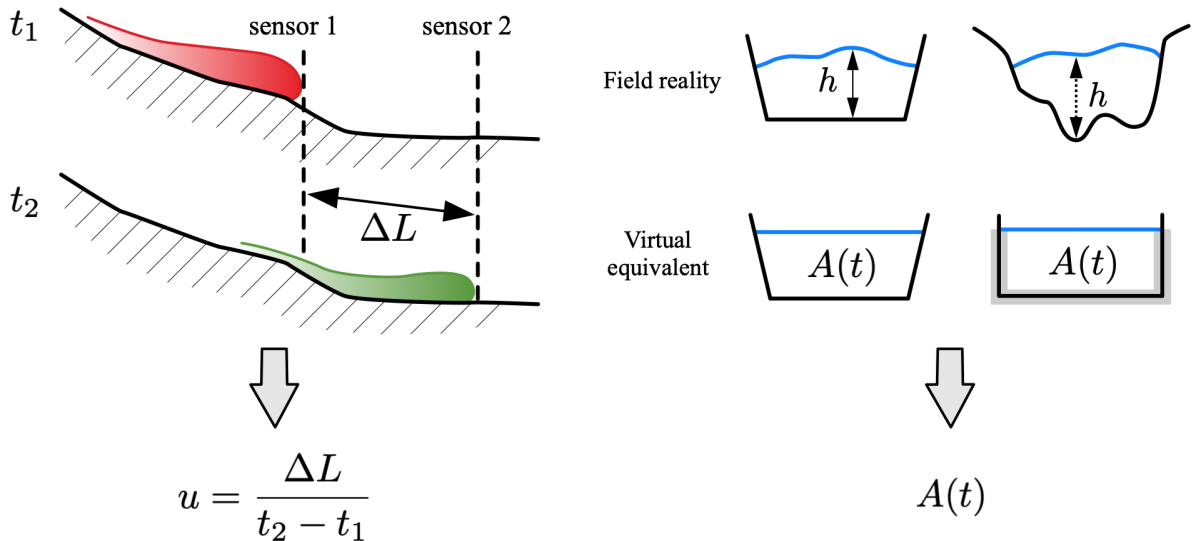


**Figure 1.** Synthetic overview of the method: a pair of sensor are used to estimate the time travel  $\Delta t$  between known locations, and a hypothesis on the cross-section shape along with the flow depth sensor are used to computed the wetted area  $A(t)$  and the associated surge parameters: discharge  $Q(t)$ , volume  $V$  and Froude number  $Fr$

## 60 2 Material and Methods

### 2.1 Approach used to compute the surge characteristics

#### 2.1.1 Concept of the event analysis

Each monitoring station has different types of sensors and different strategies to measure flow characteristics (Hürlimann et al., 2019). To apply the protocol, the following measurements are required (Fig. 1):

- 65 – flow stage measurements with representative frequency  $f$  ( $> 2\text{Hz}$ ), sufficient to detect maximum height of the flow,
- known cross section where the flow is measured, *or*, a hypothesis on the relationship between flow height and wetted area,
- a way to access directly the velocity of the surge, typically by estimating the travel time between a pair of sensors (eventually of different type) at sensible distance from one another, *or*, more accurate but rarely available, by direct
- 70 velocity measurement (e.g. image processing or large scale particle image velocimetry, see Theule et al., 2017).

These measurements must be done at sufficiently close locations to reasonably assume that the measured flow stage is associated with the measured surge velocity.

The key parameters describing the surges are then computed using these time-series:



$$Q(t) = u \cdot A(t) \quad (1)$$

75

$$V = \sum Q(t) \cdot \delta t \quad (2)$$

$$Fr = \frac{u}{\sqrt{g \cdot h_{max}}} \quad (3)$$

where  $Q$  is the debris-flow discharge [ $\text{m}^3/\text{s}$ ],  $t$  is the time [s],  $u$  is the mean surge velocity [m/s],  $A$  is the wetted section  
80 [ $\text{m}^2$ ],  $V$  is the surge volume [ $\text{m}^3$ ],  $\delta t = \frac{1}{f}$  is the time sampling interval [s],  $Fr$  is the Froude number [-],  $g$  is the gravitational  
acceleration [ $\text{m} \cdot \text{s}^{-2}$ ] and  $h_{max}$  is the maximum volume of  $h$  the flow depth [m].

### 2.1.2 Surge identification

A debris flow is generally composed of one or several surges, with eventual intermediate flows that are more diluted (called  
"diluted runoff" hereafter). The strongest complexity, destructive power, and interest in debris flows is most probably the surges  
85 and their fronts. As a consequence, the database aims at gathering measurements focusing on the surge fronts and their main  
body, rather than the full scale of the debris-flow event including several surges ( e.g. as provided in McArdell and Hirschberg,  
2020). In addition, it is arguable that diluted runoff have a lower sediment concentration and contribute much less significantly  
to the bulk event volume than the main, mature debris-flow surges. As a matter of fact, the applicability of Eqs. (1) and (2)  
90 rely on a hypothesis of high solid concentration, constant throughout the surge. Focusing data processing at the surge scale  
goes hand in hand with the intention for this database to be used to explore scientific question on the surge front behavior. This  
approach is different from other initiatives in the literature where the full scale of the event was considered.

Clearly defining the surges is thus a prerequisite to the data processing as the volume of the surge is integrated over the surge  
duration (Eq. 2), not the full event duration. If several surges in a single event are identified, each surge is taken separately as a  
data-point of the database.

95 The most basic identification of the surges is performed on the flow stage time-series by identifying surges on the flow  
hydrograph. Doing so without cross control based on other information is however doubtful on catchments where diluted  
runoff and debris floods are frequent and intense. By experience, when available, images of the front can be used to define  
this separation. Geophones data proved to enable more reliable and data-driven criteria because they capture the solid transport  
intensity (Fontaine et al., 2017; Chmiel et al., 2022). Bel (2017) showed that when mature debris flows travel at the levels of  
100 the geophones, the seismic activity is high and does not drop to zero. Conversely, immature debris-flow surges or debris floods  
may trigger seismic signal, instantaneously high, but still dropping to zero. The existence of a prolonged period of consistently  
high seismic activity can be chosen to differentiate debris-flow events from immature debris flows and debris floods. Diluted  
runoff are also easily differentiated from the surge using geophone signal.

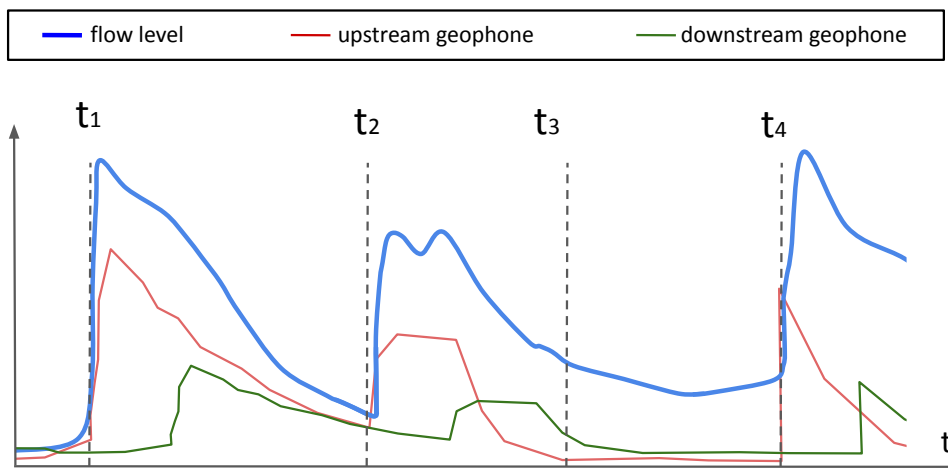


**Figure 2.** Conceptual graph explaining the surge identification approach:  $t_1$  marks the onset of the first surge : sharp increase of energy in the geophone aligned with the flow sensor and sharp increase in flow level;  $t_2$  marks the end of the first surge and the start of the second surge : geophone activity decreases before a sharp increase due to a second surge;  $t_3$  marks the end of the second surge : seismic activity is negligible even though the flow height is still high: those are the diluted runoff flows,  $t_4$  marks the start of the third surge. Note that even though the second surge has two peaks on the flow level, it is seen as one surge due to continuous seismic activity

On Fig. 2, the concept of the identification is described. The onset of a surge is detected by a sharp increase in both flow level and seismic activity, followed by a consistently non-zero seismic activity. The end of a surge is either determined by a seismic activity dropping to zero or by the onset of a second surge that can clearly be separated from the first one. Indeed, at the end of the first surge of the figure, a drop in seismic activity is clearly observed and a second sharp increase announces a second surge. On the other hand, the second surge displays two peaks in the flow level but as the seismic activity stays consistently high, those two peaks are considered part of one single surge.

### 2.1.3 Velocity calculation

In the proposed approach, as shown in Eq. (1), a single velocity value is considered for each surge. By doing so, the authors knowingly assume that the velocity is uniform within the surge. This is a crude simplification of the complex rheology of debris flows. The assumption is however required due to the lack of more precise data on most monitoring sites (see an exception in Nagl et al., 2020). This surge average velocity is a relevant proxy of the front velocity. Carefully defining the surge main body and consistently not including diluted runoff is a pivot point of this approach, as this approximation on the velocity is more relevant if the surge is only restricted to its front and main body (see section 2.1.2).

The velocity is generally computed using the lag  $\Delta t$  between the signals of two sensors and the known inter-distance  $\Delta L$  between those sensors. Once the lag is determined, the velocity is computed as  $u = \frac{\Delta L}{\Delta t}$ . Accessing the value of this lag is done by comparing the two signals and their time-scale characteristics. Choosing two sensors that are at a sensible distance one from



120 another is important: choosing two sensors too close to each other will induce significant uncertainty in the lag measurement. Due to the direct comparison of signals, the approach assumes that the source of the signal is the same that was propagating between the two different locations; in other words, the same surge is detected at both location. This approach thus also assumes that the surge does not significantly change between the two sensors e.g., no massive deposition or erosion, no strong change in surge duration, no merging between surges. However, the travel distance should be sufficiently longer than the uncertainty  
125 on the lag to provide an accurate estimate. Two methods were used to estimate velocities : cross-correlation of signals if they were good enough and a visual identification method otherwise. For more information, the detailed protocol is presented in supplementary data.

#### 2.1.4 Wetted area

From raw data, flow height and wetted area are determined at each time step. This requires assumptions on the channel bed  
130 level. Two examples will be presented in this section : assumptions that are reasonable on a check dam, and assumptions on a natural cross-section.

On controlled cross-sections, e.g., on a check dam crest, it is assumed that there is neither erosion, nor deposition. Consequently, the bed level and cross section shape are assumed constant and known. Flow height and wetted area can then easily be estimated. This configuration is preferable. Practically this means  $h_{effective} = z_{measured} - z_{dam}$ , where  $h_{effective}$  is the  
135 effective flow height [m],  $z_{measured}$  is the level of the free surface measured by the sensor [m] and  $z_{dam}$  is the check dam crest level [m].

Erosion and deposition occurring during debris-flow events may change the channel geometry. Not only does this mean that  $h_{effective} \neq z_{measured} - z_{bed}$  where  $z_{bed}$  would be the bed level before the flow [m], but it also means the cross-section shape will change during the event. The erosion-deposition process has two consequences : uncertainty on the channel shape and  
140 uncertainty on the channel bed level at a given time during the surge.

Accounting for the variability of the channel is necessary (e.g. width, bed level, shape). Cross-wise profile shape is sensitive to the event. Simplifying assumptions are necessary for cross-section shape : the simplest being the rectangular shape. Other, more precise, assumptions are to be made when information is available (e. g. trapezoidal, including knowledge of a non-erodible level on one side).

145 Bed level change throughout the surge is explored using different hypothesis (Fig. 3). With  $z_{low,min}$  the minimal bed level through the event, three hypothesis are made, when relevant :

- The whole depth of the flow is sheared (effective ) until  $z_{low,min}$  during the whole surge (**hypothesis max**),
- The flow isn't sheared in depth, this is less likely but allows to compute a minimal possible volume (**hypothesis min**),
- In the case of an erosion process, the bed level is assumed to follow a fitted logarithmic law following Kaitna and Hübl  
150 (2021) (**hypothesis ln**),

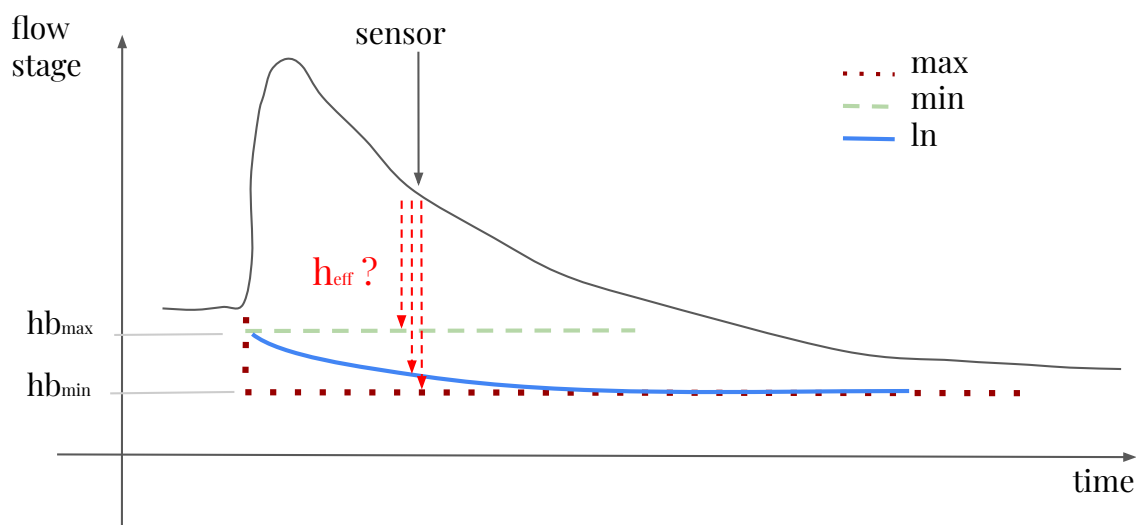


**Figure 3.** Hypotheses on the bed level used to compute the efficient flow height in a natural cross-section

## 2.2 Characteristics of the monitoring stations

The Réal Torrent, located in south of France, has been instrumented since September 2010 (Navratil et al., 2011). Three monitoring stations are distributed along the channel. Fig. 5 shows the station locations. The first one  $S_1$  is located on a 20m wide check dam as seen on Figure 8a and is the most upstream. Station  $S_2$  and  $S_3$  are located in the middle reach and at the outlet of the torrent, and are both on natural cross-sections. In Table 2, a summary of the main physical features of the stations is shown (drawn from Bel et al., 2017). The purpose of the installation is to monitor the flow stage, rainfall and seismic activity during sediment activity from bedload to debris flow. A thorough study of the station can be found in Fontaine et al. (2017) and in Bel (2017). The protocol presented above has been applied to these three stations and the results are presented further in this paper.

In essence, each station is equipped with : (i) a tipping bucket rain gauge with 0.201mm resolution (Campbell), (ii) an ultrasonic or radar flow stage sensor (Paratronic), (iii) a set of three vertical geophones (GS20DX0 Geospace) each spaced out  $\approx 100\text{m}$  apart from each other, upstream, midstream and downstream of the flow stage sensors.

Images of the channel and flow proved to be useful to facilitate the interpretation of the signals (Piton et al., 2017). Two cameras have been added to stations  $S_1$  and  $S_2$  (CC640 Campbell, replaced in 2018 by a PC900 Reconyx and EOS1200D Canon, respectively). Data are recorded using an environmental datalogger (CR1000 Campbell) powered by a solar panel, and are stored in a compact flash module (CFM100 Campbell).



**Table 1.** Physical features of the three monitoring stations

Station ID	Elevation	Drainage area	Channel width	Type of section
Units	(m a.s.l)	(km <sup>2</sup> )	(m)	
$S_1$	1450	1.3	8	Check dam
$S_2$	1340	1.7	7	Natural
$S_3$	1254	2.0	12	Natural

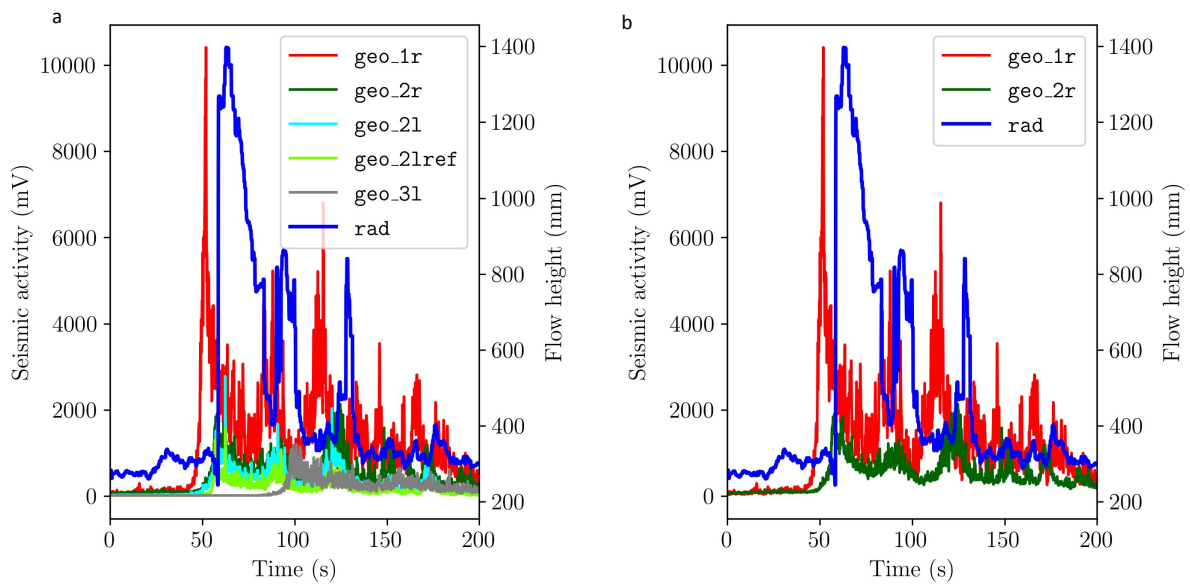


**Figure 4.** Overview of a recording of an event for station  $S_1$   $geo\_XX$  are geophone signals and  $rad$  is a flow stage signal a) Full record b) Chosen signals

On Fig. 4a, a complete set of measurements for one debris-flow event on station  $S_1$  exemplifies the data analysis on one event. Out of these raw measurements, best suited signals are chosen by the user, as seen on Fig. 4b :

- For flow height along the event, the least noisy flow stage signal is chosen. Here, only one is available (noted  $rad$  in the legend),
- For the surge identification, one geophone signal is chosen, associated with the flow stage signal. The sensors best suited for surge identification are those aligned with flow stage sensors (see Fig 5: e.g.  $geo\_2r$ ,
- For velocity determination, two geophone signals are chosen for cross-correlation. They must have the clear appearance of the debris flow behaviour, and be at a sensible distance one from each other: e.g.  $geo\_1r$  and  $geo\_2r$ .



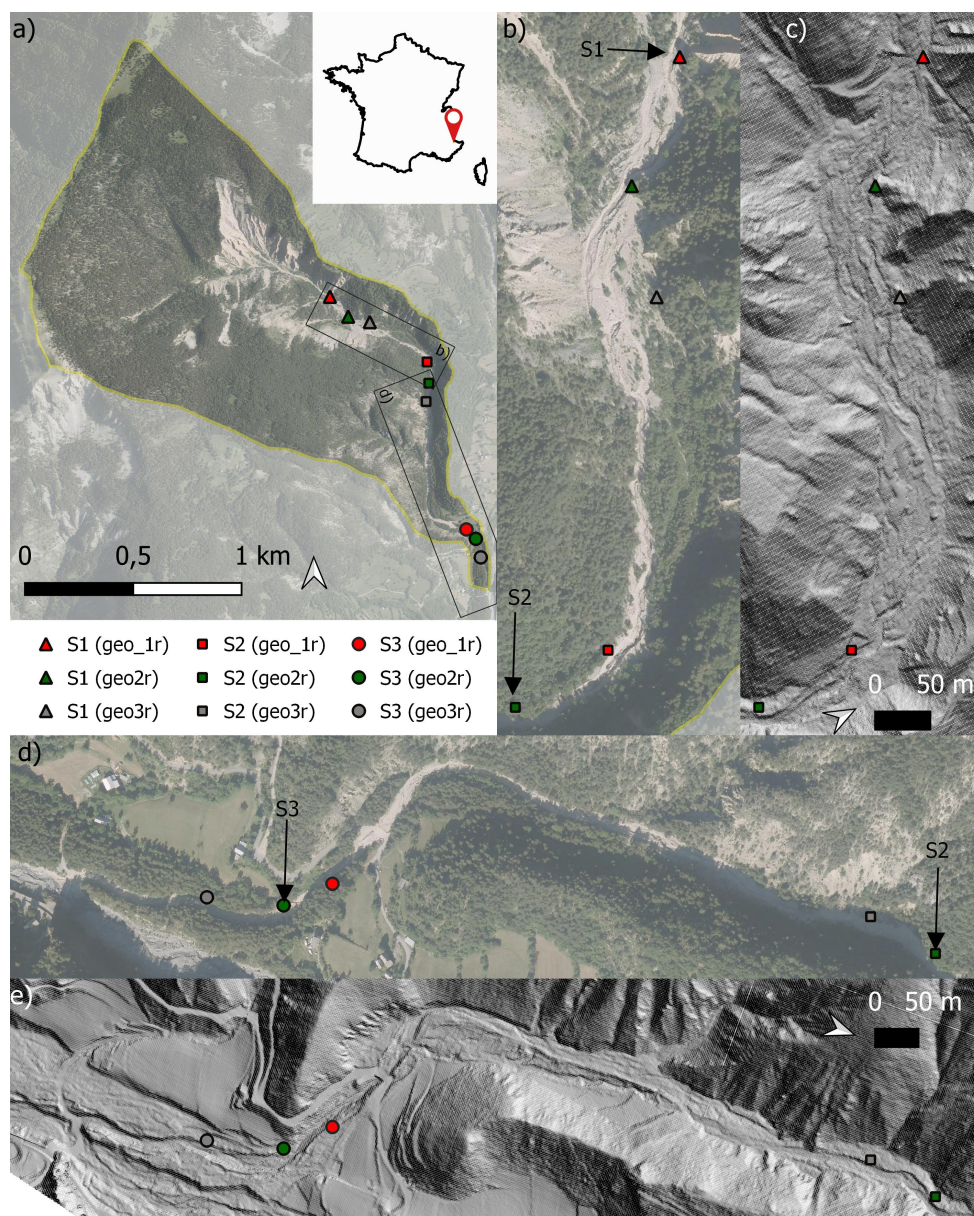


**Figure 5.** Overview of the installation on the Réal torrent : a) Full location of the torrent and its stations, drainage area is highlighted, and the three stations, arrows show the position of the flow height sensor b) Station  $S_1$  aerial photography c) Station  $S_1$  Digital Elevation Model (D.E.M.) d) Station  $S_2$  and  $S_3$  aerial photography e) Station  $S_2$  and  $S_3$  D.E.M. (aerial pictures from BD ORTHO of the french geographical survey IGN)



175 This leads to Figure 4b with only the datasets used for the determination of the hydraulic values of interest. For each of these measurements, surges are identified and their features are computed. The user cross-controls the measurements and eventually goes for the visual method if the cross-correlation does not provide satisfying results (irrelevant value of velocity, low correlation coefficient or inconsistent velocity when compared to a first quick manual computation). This visual method was used marginally, i.e. for one surge in our case, and was confirmed using image processing.

180 These sensors and post-processing allow to have for each event the followings : (i) seismic activity at three different points around the station with a frequency of 5 or 10Hz, (ii) rainfall data every 5mn, (iii) flow stage with a frequency of 5 or 10Hz, and (iv) imagery of the event (when possible) with a 0.2 or 1Hz frequency,

### 3 Results

#### 3.1 Summary of available data

185 For the construction of the database, only significant events were considered to ensure the analysis of mature debris flows: a threshold of flow stage above 1 m was selected for this catchment. Overall, 34 events were considered for the Réal station for the period 2011-2020. Table 2 show when those events occurred, the number of surges passing at each station and the availability of the describing parameters. Over the 34 surges, most, i.e. 26, are recorded in the upstream station  $S_1$ , while only four surges reached  $S_2$  and only two reached  $S_3$ , the most downstream station. The lack of events on the period 2014 - 2018 is  
190 partially due to the natural variability of event sizes but also due to faulty sensors during that time period.

#### 3.2 Distribution of surge parameters

One of the main interests of having an integrative dataset is to allow access to field ranges of hydraulic values of interest, such as Froude numbers and volumes of surges. In Fig. 6, different cumulative distribution functions (CDF) of the data-sets are presented. Froude numbers range from 0.3 to 1.6, showing the range of regimes found in debris flows in our site. Whether this  
195 is a site specific feature or it can be shown on more sites that Froude number are typically critical would be a strong take home message for the community.

Surge volumes range from 200 to 4500 m<sup>3</sup> (Fig. 6c - quantile 25%, 50%, 75%: 390 m<sup>3</sup>, 640 m<sup>3</sup>, 1460 m<sup>3</sup>). Surges are relatively small, typically from 1000 to 2000 m<sup>3</sup>/km<sup>2</sup> (recall that this is surge scale and an event may comprise several of them, e.g., 1 - 4 in our observations of Table. 2, and some diluted runoff). Maximal flow stage is most of the time lower than  
200 2m (Fig. 6a - quantile 25%, 50%, 75%: 1.1m, 1.25m, 1.6 m). The peak discharge range between 6.2 and 91.8 m<sup>3</sup>/s (Fig. 6b - quantile 25%, 50%, 75%: 10.8 m<sup>3</sup>/s, 17.5 m<sup>3</sup>/s, 27.9 m<sup>3</sup>/s). The unit peak discharge is thus typically 0.775 to 7.65 m<sup>3</sup>/s. Finally, Froude numbers range from 0.25 to 1.6 (Fig. 6d - quantile 25%, 50%, 75%: 0.48, 0.65, 0.95), i.e. are typically near critical. The complete dataset is available in the supplementary data on Table S1.

Finally, relationships between these hydraulic values may be explored with a wider dataset, and a more thorough description  
205 of each event. Fig. 7 shows for instance the relationship between a few key variable (Froude numbers, volume of each surge



**Table 2.** Summary of the available data : black cells corresponds to available data, gray is non-applicable and crossed out cells are event that were detected but for which the data was not retrieved due to faulty sensors

Date	Nb surge			Volume			Peak discharge			Froude number			Maximum height		
	S <sub>1</sub>	S <sub>2</sub>	S <sub>3</sub>	S <sub>1</sub>	S <sub>2</sub>	S <sub>3</sub>	S <sub>1</sub>	S <sub>2</sub>	S <sub>3</sub>	S <sub>1</sub>	S <sub>2</sub>	S <sub>3</sub>	S <sub>1</sub>	S <sub>2</sub>	S <sub>3</sub>
2011-06-29	1	1	1												
2011-09-17	1	1													
2012-04-30	4	1													
2012-05-27	1														
2013-03-30	1	1													
2013-05-18	3														
2013-07-22	1														
2014-01-04	1														
2014-06-10	1		1												
2014-09-20	1	1			x		x			x			x		
2018-10-29	1		1			x		x			x			x	
2019-12-01	2														
2019-12-19	4														
2019-12-20	1														
2019-12-21	1														
2020-06-07	1														
2020-06-13	1														
Total number of surges	34			26	4	2									

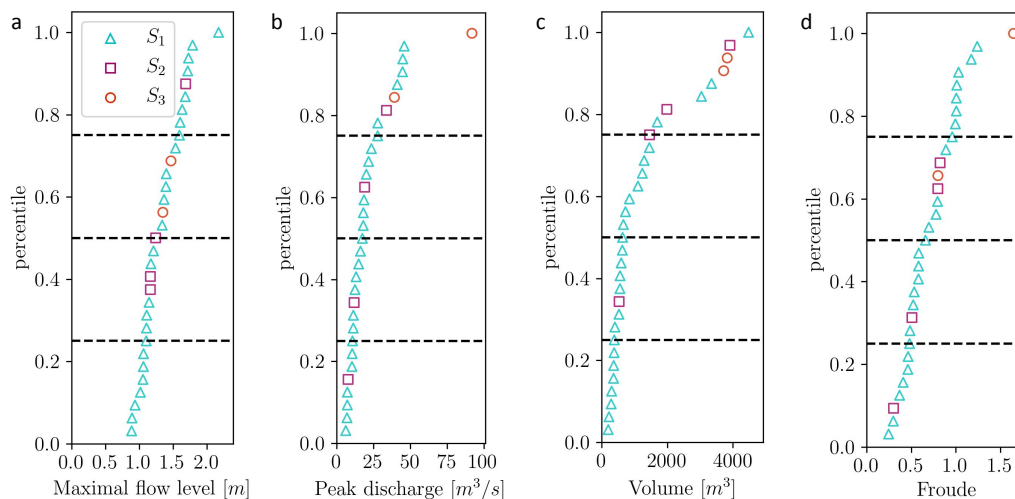


**Figure 6.** Cumulative density functions of hydraulic values of interest : a) Maximal flow level, b) Peak discharge, c) Volume, d) Froude

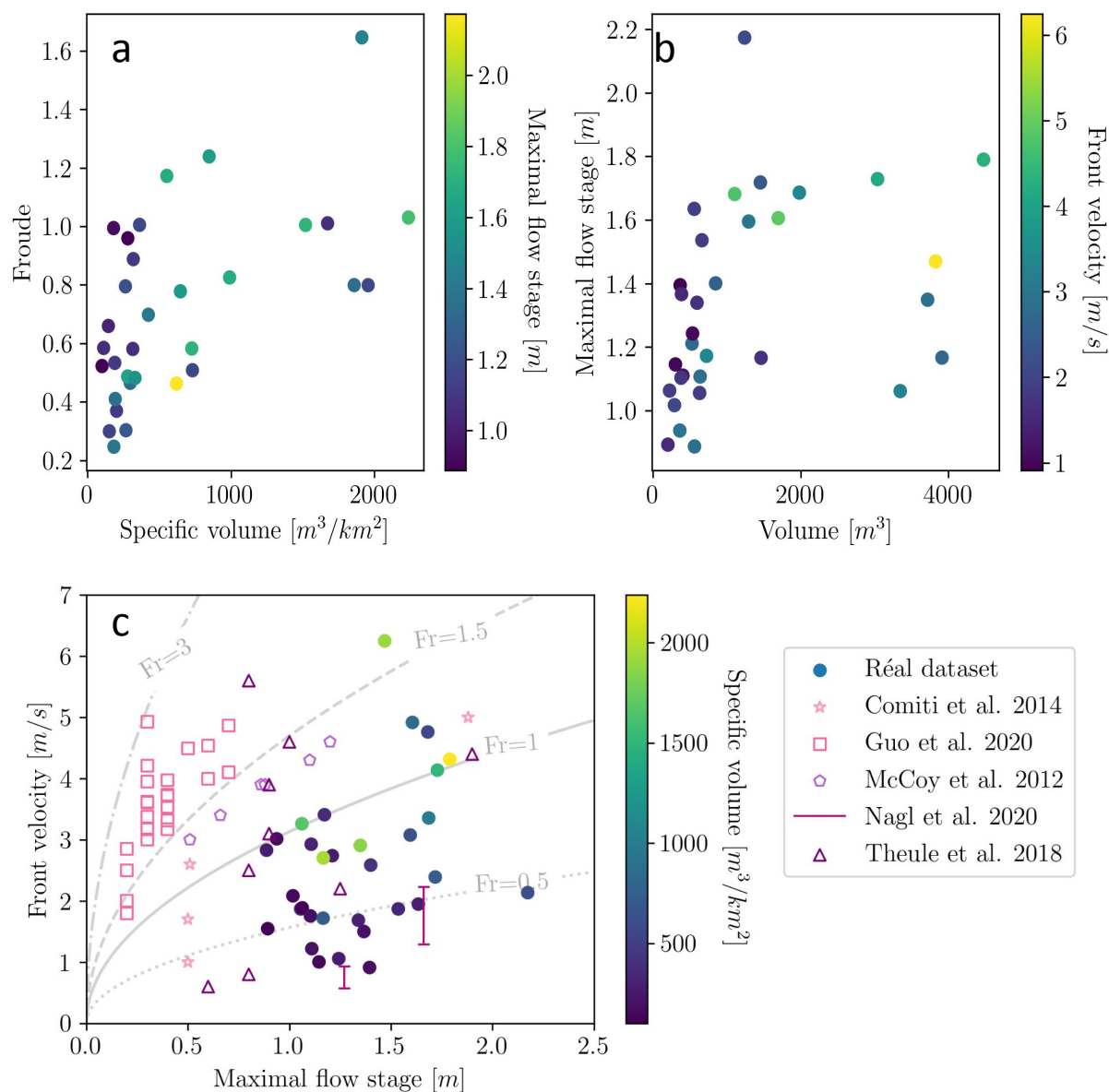


**Figure 7.** Examples of different relationships that can be explored with this dataset: a) Froude number VS specific surge volume, b) Maximum flow stage VS surge volume and c) Front velocity VS maximum flow stage. Data from the litterature is displayed on c) to contextualize the values: For Nagl et al. 2020 ranges of maximal and minimal values were taken. Colormapping is only showed for the Réal dataset. Grey lines display different Froude number relationships.



normalized by the catchment area, front height and velocity). To cross-compare measurements performed at different stations, but also to help transferring these results to other catchments, the surge volume was normalized by the catchment area. A slight trend can be seen on Fig. 7a with increasing Froude number for increasing specific surge volume. Maximum flow stage is quite variable with surge volume (Fig. 7b). Similarly, no clear correlation seems to appear between front velocity and flow stage (Fig. 7c). Literature data has been displayed, drawing from Comiti et al. (2014); Guo et al. (2020); McCoy et al. (2012); Nagl et al. (2020); Theule et al. (2018).

We interpret these lack of trend as evidences of varying surge viscosity between events. The sample size remains however relatively small and site-specific, calling for prudent interpretation of these data. We believe it will be of high interest if several other sites could be added to a similar analysis. Fitting a relationship between Froude numbers and surge volume could be a very interesting asset for numerical and experimental modeling.

## 4 Discussion

### 4.1 Relationship between surge parameters

Figure 6 and 7 show the ranges of the different features in the database for the Réal torrent. Specific volumes range from  $156m^3/km^2$  to  $3342m^3/km^2$ . In comparison to specific volumes given by McArdell and Hirschberg (2020), which range from  $171m^3/km^2$  to  $7690m^3/km^2$ , these are much smaller. One of the key reason why there is such a difference -apart from differences in geological and rheological makeup- is the method employed : classically, available volumes can contain multiple surges and diluted tails and thus, volumes are not as restrictive as in the method employed in this paper. Specific volumes of the Réal catchment being much smaller is consistent with the difference in hypothesis in each methods. In Comiti et al. (2014), the Gatria catchment monitoring is described and the method employed is much more comparable. In that case, specific volumes for the two events are  $380m^3/km^2$  and  $1500m^3/km^2$ , which show similar range to our dataset.

Several literature values are added on Fig. 7c. Our dataset ranges in similar Froude numbers as the literature, with most points between  $Fr = 0.5$  and  $Fr = 1.5$ . A point from Simoni et al. (2020) has not been displayed for clarity of the Figure. They provide maximal values of velocity ( $4m/s$ ) and flow depth ( $4.5m$ ) for one event, rendering a subcritical Froude number ( $Fr = 0.6$ ). The dataset provided by Guo et al. (2020) has generally higher Froude numbers. This is attributed to the specific rheology of debris-flows in this catchment which do not have the slow laminar features that can be found on reach like the Réal torrent. Overall, all Froude numbers displayed stay under  $Fr = 3$ .

On Fig. 7a, while no clear trend can be drawn, there are no surges with large specific volumes ( $> 1000m^3/km^2$ ) which have clearly subcritical Froude numbers (all Froude numbers are above 0.8). Most of these surges have near critical Froude numbers. The absence of subcritical Froude numbers can be seen as such heavy and large surges requiring a strong inertial input to flow. On the other hand, smaller surges can flow more easily and do not need strong inertial inputs to maintain steady flow. The fact that most of these surges are near critical might in part be due to the sampling at the stations and not the possibility for them to exist : very heavy and very fast surges with high volume and high inertia are very rare with the topography of this



catchment, so the surges with high volume that are passing at the stations meet the "minimum requirements" to flow. One surge with supercritical Froude number and high volume is still detected.

240 For smaller specific volumes ( $< 1000m^3/km^2$ ), Froude numbers range from 0.2 to 1.2 with most surges being clearly subcritical with Froude  $< 0.8$ . Flow conditions for smaller volumes require less inertial input. For a same specific volume, a wide range of subcritical Froude numbers are found, showing that volume is not the main driver to flowing conditions, and that surge viscosity vary widely in surges with low volume, i.e.  $< 1000m^3/km^2$ .

245 The initial expectation for Figure 7b would be that surges of higher volume render higher maximal flow stage. This would be the case if hydrograph shape was consistent on all events. The lack of clear relationship between the two features highlights the complexity of debris flow surges : surges with the highest volumes can be caused by short very high flows or longer more moderate flows. There is a great variety of hydrograph shapes at surge scale.

250 Figure 7c shows no definitive relationship between witnesses of inertial and potential inputs in the flow. This is yet another argument to point out that surge granular content and viscosity might differ widely from one event to another on the same catchment. The idea that composition of the debris flow surges changes between events is supported by Hürlimann et al. (2003). A study of the surge content in boulders and coarse grain (Takahashi, 2014) and of their interstitial fluid rheology (Bardou et al., 2003) would be complementary to support this idea, but is at the moment not possible with the available data.

#### 4.2 Evidence of the erosion/deposition cycles

255 On Fig. 5b and d, the valley bottom landforms bear the footprint of high morphological activity due to debris flows. More specifically in the reach between  $S_1$  and  $S_2$  where landforms such as abandoned channels, levees and lobes can be seen (Fig. 1b-c). Fig. 8 exemplifies these changes in the channel morphology directly downstream of station  $S_1$  at five different dates. An erosion/deposition cycle of the channel incising and refilling is highlighted over six years of field pictures. Such processes explain why many debris flows are measured at station  $S_1$  while much less are observed further downstream.

260 In Figure 9, volumes of all events are shown along time. If the geomorphic cycle exemplified in Figure 8 was detectable by this method, pseudo-cycles of cumulated volumes surges at station  $S_1$  would be less frequently exported as surges of higher volume at station  $S_2$  (or as many small volume surges at  $S_2$  in the following years). It can be seen that the two surges reaching station  $S_3$  are indeed of relatively high volume but the data lacking between 2015 and 2019 prevent us to draw further observations. With the current data, we can simply conclude that higher volumes of debris flows pass station  $S_1$  than further downstream. The system is thus either or both storing sediment in the valley through aggradation and/or also exporting 265 sediment volume through another process than mature debris flows. The applicability of this approach to study the sediment cascade is limited by multiple aspects: the first being that the data of interest is kept at the surge scale and focus on mature debris flows (threshold height  $> 1$  m). Due to the way the data has been processed, studies on global sediment balance are not possible with this analysis, as the events of bed-load and wash-load are not taken into account. Indeed, despite its high debris-flow activity, the Réal Torrent experience other processes causing long term morphological changes as bed-load transport and 270 debris flood that have meaningful impact on morphological changes and sediment fluxes in various parts of the catchment (Theule et al., 2012).



**Figure 8.** Pictures taken on the  $S_1$  stations over 6 years a) channel filled in June 2009, b) channel deeply incised in July 2011, c) channel widened and partially refilled in June 2014, d) channel further incised October 2014, e) channel refilled in July 2014 (pictures from the authors)

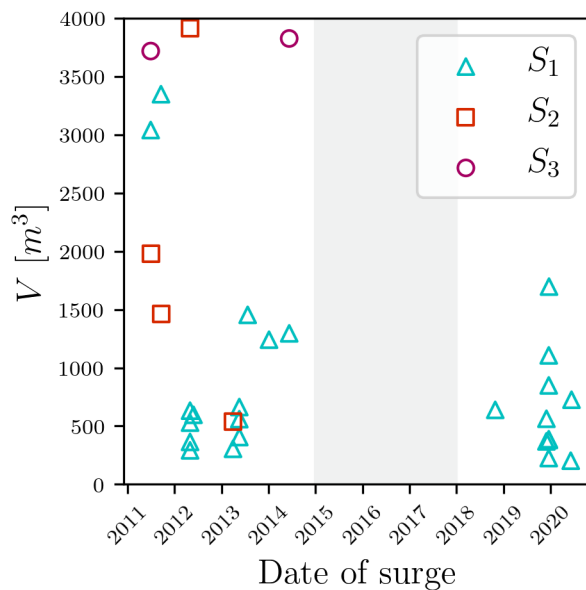


**Figure 9.** Volume of the surges of mature debris flow passing the stations, grey area has no data partly due to a faulty sensor invalidating measurements from 2016 until the end of 2017 when the sensor was replaced. No surges were detected in 2015.

### 4.3 Upstream-downstream transfers of debris-flow surges along the channel

A key interest of having three different monitoring stations on the same torrent is the possibility to study cascading sediment transfers. Fig. 10 shows the analysis of volumes, flow rates, Froude numbers and flow height of each events that could be found on more than one of the station. One could expect to see consistent relationships between upstream and downstream characteristics but results are more complicated.

Volumes passing stations  $S_1$ ,  $S_2$  and  $S_3$  are generally very different at a same date (Fig. 10). In some cases, the debris-flow surges were growing, recruiting sediment from the bed ( $V_2 > V_1$  and / or  $V_3 > V_2$ ) showing the profound morphological changes debris flow passage can lead to. In other cases, some deposition occurred ( $V_2 < V_1$ ) but erosion might still appear downstream. For the subset of events happening on the same date at the three stations, no particular relationship between the four parameters studied in Fig. 7 was identified.

On Fig. 10a and b, volumes and peak discharge should consistently grow if the surges were consistently eroding from upstream to downstream of the reach. Events like the 2012-04-30 surges show increasing volumes, with a potential agglomeration of the surges between  $S_1$  and  $S_2$  (accumulated volumes at  $S_1$  are smaller than the volume at  $S_2$ ). This shows deep erosion is possible between the two stations, which is consistent with the morphological changes shown on Figure 5b. Nonetheless, on this event, peak discharge is not increasing between the two stations.

Similarly, maximum surge depth can also either be lower upstream (2013-03-30 of Fig. 10c) or higher at the first station (events of summers 2011 and 2014, Fig. 10c). The Froude number also varies from upstream to downstream with some events



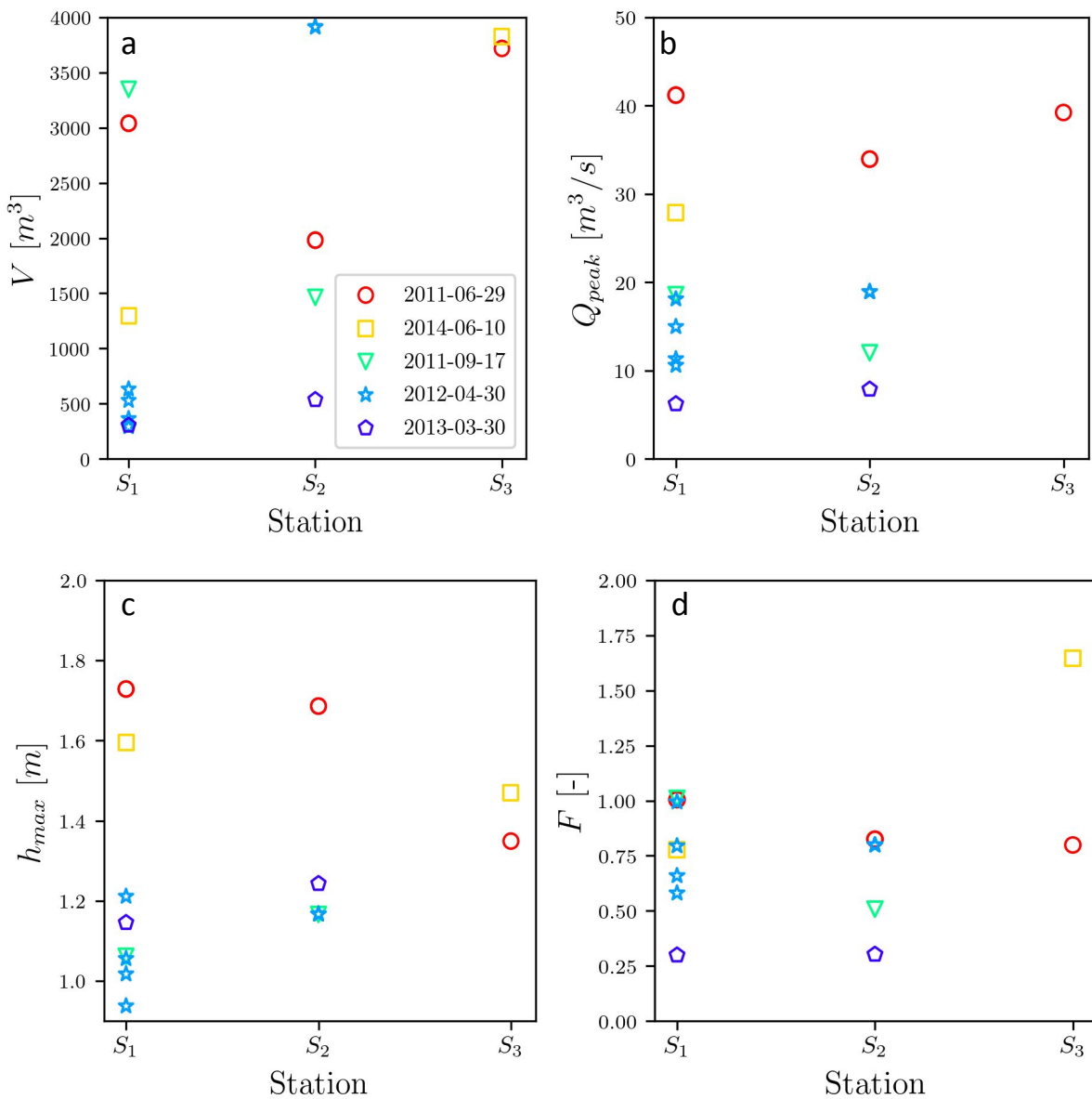


**Figure 10.** Temporal study for surges detected at two different stations a) Peak discharge over traveled distance (from the beginning of the channel), b) Volume over traveled distance c) Maximum flow level and d) Froude number



having lower downstream Froude number and others not (Fig. 10d). Froude numbers could be expected to be consistent from  
290 upstream to downstream : the ability to flow of the surge would be driven by the interplay between kinetic and potential inputs.  
Erosion and deposition processes of the surge along the reach will influence the Froude number both by changing the volume  
and the composition (and viscosity) of the surge.

The observation on volumes, discharges and surge heights, as well as the much stronger frequency of mature debris flow  
passing  $S_1$  against those passing  $S_2$  or  $S_3$  (26, 4 and 2, respectively), highlight that strong processes of erosion and deposition  
295 occur in the catchment.

While analysing data from three different stations located on such a small and active catchment is interesting, events detected  
on multiple stations are scarce : most surges detected upstream tend to deposit or to attenuate while travelling such that they  
are not detected as a mature surge downstream. On the opposite end of this spectrum, a surge that was under the detection  
threshold on the upstream station might have become fully formed in the downstream stations (see the events of June 10, 2014  
300 and October 28, 2018 that were detected at  $S_1$ , not at  $S_2$  and again detected at  $S_3$ , Tab. 2).

On the other hand, surges that are detected on multiple stations are also difficult to rely to each other, and although volume  
comparison could be interesting, actual quantitative comparison relies on the hypothesis that the exact same surge between  
upstream and downstream stations is comparable, i.e. that along the journey, only marginal changes in process occurred,  
which is known to be a crude hypothesis of this first work. In essence, the data shown in this paper are interesting because  
305 they are actual field observations with quantitative measurements but the analysis of the catchment sediment transfers is not  
possible. However, the dataset does demonstrate how strong and intense the processes of erosion and deposition in debris flow  
prone catchments are. An analysis seeking to determine rainfall triggering conditions of debris flows would for instance draw  
different conclusions depending on which station is used (but see Bel et al., 2017, which partially addresses this issue). We  
believe that further effort should be put on better understanding not only debris-flow triggering factor but also propagation  
310 through headwaters and intermediate reaches.

#### 4.4 Analysis of the physical ranges of the events

Comparing the present data to the literature shows the ranges found in the Réal torrent to be consistent with empirical fits pro-  
posed in previous works (Bovis and Jakob, 1999; Rickenmann, 1999; Mizuyama et al., 1992), even though the measurements  
of volumes were done with debris-flow levees in these previous works rather than direct measurements as our contribution.  
315 According to Fig. 11, the peak discharge of the Réal catchment for various volumes of debris-flow surges seems closer from  
the empirical fit related to granular debris flows of Bovis and Jakob (1999) or the fit proposed by Rickenmann (1999). Peak  
discharges associated with muddy debris flows are lower than those measured at the Réal catchment for equivalent volumes.  
These results are consistent with the work of Bel (2017) who already showed this concordance using an analysis considering  
the full debris-flow event with a former version of this protocol.

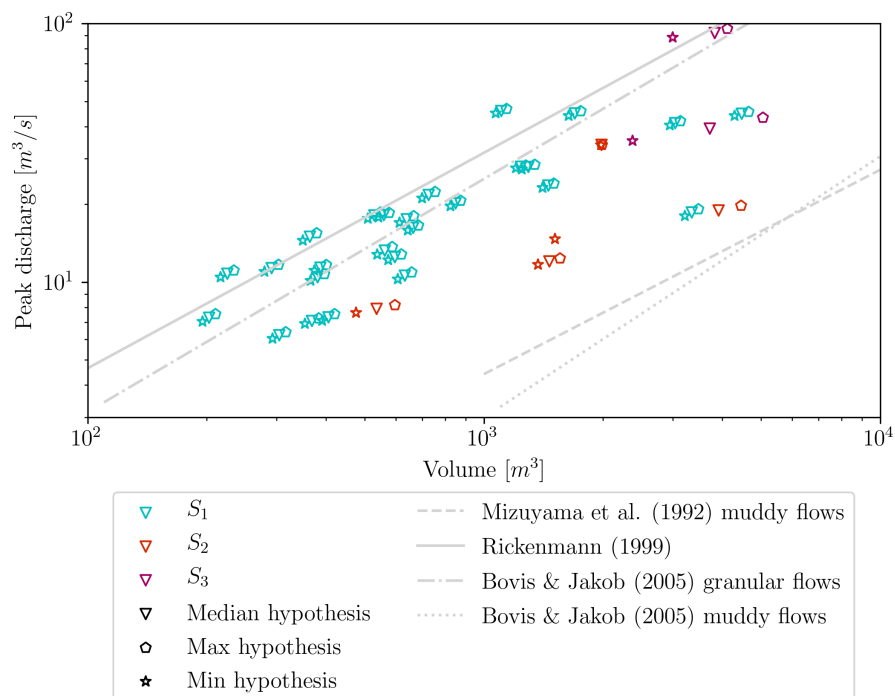


**Figure 11.** Relationship between debris-flow volume and peak discharge for all three stations of the Réal torrent (color scale for the station and dot shape for the hypothesis on the bed level) - Comparison with empirical fits of datasets from the literature (Bovis and Jakob, 1999; Rickenmann, 1999; Mizuyama et al., 1992)



## 320 5 Conclusions

This work is a proof of concept for data processing of debris-flow surges from monitoring stations. A full and simple protocol on debris-flow data processing is presented. The clear goal of this paper is not only to make a first dataset available but also to call for collaboration on a common database for debris-flow surge features.

325 Bulk surge features are investigated including volume, front height, peak discharge and Froude number. This investigation allowed to access these hydraulic features on 34 surges gathered from 2011 to 2020 on the Réal torrent catchment (South-East France, catchment size 1.3 - 2 km<sup>2</sup>). Surge volumes are typically a few thousand cubic meters, peak flow heights range from one to two meters, peak discharge is usually of the order of magnitude of a few dozens of cubic metres per second and their Froude number is near critical.

330 Access to representative field data will ensure accurate representation of these natural flows. This database is meant to be extended to other monitoring stations to strongly gain in impact on the scientific community. Open access to field data for numerical research can be the bridge needed to close any gaps between the field-driven approaches and the numerical investigations. Research on debris flow behaviour is growing and we hope that this initiative will allow more projects to be born, and allow field observations and numerical computations to evolve conjointly. On top of this, experiences drawn from the post processing of such data can allow for better, more effective data monitoring in the future (e.g. what type of cross section  
335 to choose, where to install successive stations).

*Data availability.* The processed data is available in the supplementary data of this paper. The raw data (geophone signals, flow sensors and rain accumulation) are available upon reasonable requests to the authors

*Author contributions.* Conceptualization: S.L. and G.P., data curation: S.L. and F.F., Methodology: S.L., F.F. and G.P., Supervision: F.L. and G.P., Visualization: S.L., V.R. and G.P., Writing - original draft preparation: all authors.

340 *Competing interests.* The authors declare that they have no conflict of interest.

*Acknowledgements.* The work of S.L., V.R. and G.P. was supported by the LabEx Tec21 Investissements d'avenir - agreement n°ANR-11-LABX-0030. F.F. and F.L. were supported by the Labex OSUG@2020 (Investissements d'Avenir, grant agreement ANR-10-LABX-0056).



## References

- Albaba, A., Lambert, S., Nicot, F., and Chareyre, B.: Modeling the Impact of Granular Flow against an Obstacle, in: Recent Advances in  
345 Modeling Landslides and Debris Flows, edited by Wu, W., pp. 95–105, Springer International Publishing, 2015.
- Bardou, E., Ancey, C., Bonnard, C., and Vulliet, L.: Classification of debris-flow deposits for hazard assessment in alpine areas, in: 3th  
International Conference on Debris-Flow hazards mitigation : mechanics, prediction, and assessment., pp. 799–808, Millpress, 2003.
- Bel, C.: Analysis of debris-flow occurrence in active catchments of the French Alps using monitoring stations, Ph.D. thesis, Université  
Grenoble Alpes, 2017.
- 350 Bel, C., Liébault, F., Navratil, O., Eckert, N., Bellot, H., Fontaine, F., and Laigle, D.: Rainfall control of debris-flow triggering in the Réal  
Torrent, Southern French Prealps, *Geomorphology*, 291, 17–32, 2017.
- Bovis, M. J. and Jakob, M.: The role of debris supply conditions in predicting debris flow activity, *Earth Surface Processes and Landforms*,  
24, 1039–1054, 1999.
- Ceccato, F., Redaelli, I., di Prisco, C., and Simonini, P.: Impact forces of granular flows on rigid structures: Comparison between discontin-  
355 uous (DEM) and continuous (MPM) numerical approaches, *Computers and Geotechnics*, 103, 201–217, 2018.
- Chen, J., Wang, D., Zhao, W., Chen, H., Wang, T., Nepal, N., and Chen, X.: Laboratory study on the characteristics of large wood and debris  
flow processes at slit-check dams, *Landslides*, 17, 1703–1711, <https://doi.org/10.1007/s10346-020-01409-3>, 2020.
- Chmiel, M., Godano, M., Piantini, M., Brigode, P., Gimbert, F., Bakker, M., Courboulex, F., Ampuero, J.-P., Rivet, D., Sladen, A., Ambrois,  
D., and Chapuis, M.: Brief communication: Seismological analysis of flood dynamics and hydrologically triggered earthquake swarms  
360 associated with Storm Alex, *Natural Hazards and Earth System Sciences*, 22, 1541–1558, <https://doi.org/10.5194/nhess-22-1541-2022>,  
2022.
- Comiti, F., Marchi, L., Macconi, P., Arattano, M., Bertoldi, G., Borga, M., Brardinoni, F., Cavalli, M., D’agostino, V., Penna, D., et al.: A new  
monitoring station for debris flows in the European Alps: first observations in the Gadria basin, *Natural hazards*, 73, 1175–1198, 2014.
- Faug, T., Caccamo, P., and Chanut, B.: A scaling law for impact force of a granular avalanche flowing past a wall, *Geophysical Research*  
365 *Letters*, 39, 1–5, <https://doi.org/10.1029/2012gl054112>, 2012.
- Fontaine, F., Bel, C., Bellot, H., Piton, G., Liébault, F., Juppet, M., ., and Royer, K.: Suivi automatisé des crues à fort transport solide dans les  
torrents : stratégie de mesure et potentiel des données collectées, in: *Monitoring en milieux naturels - Retours d’expériences en terrains  
difficiles*, vol. 19, pp. 213–220, Collection EDYTEM, <https://hal.archives-ouvertes.fr/hal-01656535>, 2017.
- Goodwin, G. R. and Choi, C. E.: A depth-averaged SPH study on spreading mechanisms of geophysical flows in debris basins: Implica-  
370 tions for terminal barrier design requirements, *Computers and Geotechnics*, 141, 104 503, <https://doi.org/10.1016/j.compgeo.2021.104503>,  
2022.
- Guo, X., Li, Y., Cui, P., Yan, H., and Zhuang, J.: Intermittent viscous debris flow formation in Jiangjia Gully from the perspectives of  
hydrological processes and material supply, 589, <https://doi.org/10.1016/j.jhydrol.2020.125184>, 2020.
- Hürlimann, M., Rickenmann, D., and Graf, C.: Field and monitoring data of debris-flow events in the Swiss Alps, *Canadian Geotechnical*  
375 *Journal*, 40, 161–175, <https://doi.org/10.1139/t02-087>, 2003.
- Hürlimann, M., Coviello, V., Bel, C., Guo, X., Berti, M., Graf, C., Hübl, J., Miyata, S., Smith, J. B., and Yin, H.-Y.: Debris-flow monitoring  
and warning: Review and examples, *Earth-Science Reviews*, 199, 102 981, 2019.
- Jakob, M. and Hungr, O.: *Debris-flow Hazards and Related Phenomena*, Springer Praxis Books, Springer Berlin Heidelberg, 2005.



- Kaitna, R. and Hübl, J.: Monitoring debris-flow surges and triggering rainfall at the Lattenbach creek, Austria, *Environmental and Engineering Geoscience*, 2021.
- 380 Laigle, D. and Labbe, M.: SPH-Based Numerical Study of the Impact of Mudflows on Obstacles, *International Journal of Erosion Control Engineering*, 10, 12, 2017.
- McArdell, B. W. and Hirschberg, J.: Debris-flow volumes at the Illgraben 2000-2017, *EnviDat*, 2020.
- McCoy, S. W., Kean, J. W., Coe, J. A., Tucker, G. E., Staley, D. M., and Wasklewicz, T. A.: Sediment entrainment by debris flows: In situ  
385 measurements from the headwaters of a steep catchment, 117, <https://doi.org/10.1029/2011JF002278>, 2012.
- Mizuyama, T., Kobashi, S., and Ou, G.: Prediction of debris flow peak discharge, in: *Symposium Proceedings of the INTERPRAENENT 1992 - BERN*, pp. 99–108, 1992.
- Nagl, G., Hübl, J., and Kaitna, R.: Velocity profiles and basal stresses in natural debris flows, *Earth Surface Processes and Landforms*, 45, 1764–1776, 2020.
- 390 Navratil, O., Liébault, F., Bellot, H., Theule, J., Ravanat, X., Ousset, F., Laigle, D., Segel, V., and Fiquet, M.: Installation d'un suivi en continu des crues et laves torrentielles dans les Alpes françaises, in: *Journée de Rencontre sur les Dangers Naturels*, Institut de Géomatique et d'Analyse du Risque, pp. 8–p, 2011.
- Ng, C. W. W., Liu, H., Choi, C. E., Kwan, J. S. H., and Pun, W. K.: Impact dynamics of boulder-enriched debris flow on a rigid barrier, *Journal of Geotechnical and Geoenvironmental Engineering (ASCE)*, [https://doi.org/10.1061/\(ASCE\)GT.1943-5606.0002485](https://doi.org/10.1061/(ASCE)GT.1943-5606.0002485), 2020.
- 395 Piton, G., Berthet, J., Bel, C., Fontaine, F., Bellot, H., Malet, E., Astrade, L., Recking, A., Liébault, F., Astier, G., Juppet, M., and Royer, K.: Dynamique géomorphologique des torrents : intérêt de l'emploi des appareils photographiques automatiques, in: *Monitoring en milieux naturels - Retours d'expériences en terrains difficiles*, vol. 19, pp. 205–212, Collection EDYTEM, <https://hal.archives-ouvertes.fr/hal-01635571>, 2017.
- Rickenmann, D.: Empirical relationships for debris flows, *Natural hazards*, 19, 47–77, 1999.
- 400 Simoni, A., Bernard, M., Berti, M., Boreggio, M., Lanzoni, S., Stancanelli, L. M., and Gregoretti, C.: Runoff-generated debris flows: Observation of initiation conditions and erosion–deposition dynamics along the channel at Cancia (eastern Italian Alps), 45, <https://doi.org/10.1002/esp.4981>, 2020.
- Suwa, H., Okano, K., and Kanno, T.: Forty years of debris flow monitoring at Kamikamihorizawa Creek, Mount Yakedake, Japan, in: *5th international conference on debris-flow hazards mitigation: mechanics, prediction and assessment*. Casa Editrice UniversitaLa Sapienza, 405 Roma, pp. 605–613, 2011.
- Takahashi, T.: *Debris flow: mechanics, prediction and countermeasures*, CRC Press, 2nd edition edn., 2014.
- Theule, J., Liébault, F., Loye, A., Laigle, D., and Jaboyedoff, M.: Sediment budget monitoring of debris-flow and bedload transport in the Manival Torrent, SE France, *Natural Hazards and Earth System Science*, 12, 731–749, <https://doi.org/10.5194/nhess-12-731-2012>, 2012.
- Theule, J., Crema, S. C., Marchi, L., Cavalli, M., and Comiti, F.: Exploiting LSPIV to assess debris-flow velocities in the field, *Natural  
410 Hazards and Earth System Sciences*, 18, 1–13, 2017.
- Theule, J. I., Crema, S., Marchi, L., Cavalli, M., and Comiti, F.: Exploiting LSPIV to assess debris-flow velocities in the field, 18, 1–13, <https://doi.org/10.5194/nhess-18-1-2018>, 2018.